

## **Test Results for the 80 First Article samples of the Hamamatsu S10943-0258(X) array**

F. Barbosa, J.E. McKisson, J. McKisson, Y. Qiang, E. Smith, C. Zorn  
Jefferson Laboratory  
Newport News, VA 23606

### **Abstract**

Eighty samples of the model S10943-0258(X) SiPM arrays were received from Hamamatsu. All specifications were successfully achieved except for two which were not included in this set of tests – *sensitivity to magnetic fields* and *sensitivity to radiation*. These are discussed separately in the final section of the report. All of the key parameters were met or exceeded as shown in Table 1 of the report.

It is recommended that full production of the S10943-0258(X) devices proceed as outlined in the original contract (JSA-11-C0365).

## Introduction and Initial Examination

On March 8, 2011, the full set of 80 1<sup>st</sup> Article SiPM arrays arrived at Jefferson Laboratory (JLAB). The samples were packaged into individual static-free ziplock bags with identity tags glued to each bag. The tag include the model (S10943-0258(X)) and the serial number (1–96). The serial number is also stamped in one corner of the SiPM. The serial numbers were consecutive excepting a total of 16 that were withheld by Hamamatsu presumably due to QC requirements. In addition, the sample set was divided into 2 sets, each set of 40 packed carefully in successive layers of 10 samples in a static-free plastic box. Hamamatsu provided data both in paper and digital form. For each sample, an operating voltage ( $V_{op}$ ) and Dark Rate (MHz) was provided for each of the 16  $3 \times 3$  mm<sup>2</sup> cells of each array. These were provided assuming a standard Gain of  $7.5 \cdot 10^5$  and an ambient temperature of 25°C. Some supplementary data was also provided, including (a) PDE for a single cell for 12 samples (7 of which are among the JLAB set), (b) a detailed PDE map of one sample which covers both a range of wavelengths and all the cells, and (c) some miscellaneous data on crosstalk and pulse shape for some samples.

Figure 1 is a schematic provided by Hamamatsu showing the geometrical layout of an array. The pinout pattern shows that, in addition to a separate output from each of the 16  $3 \times 3$  mm<sup>2</sup> cells, a separate bias can be applied to adjacent sets of 4 cells clustered in a quadrant. For these tests, as well as for the actual operation of the devices, all cells received the same applied bias. This operating voltage ( $V_{op}$ ) was taken as the arithmetic average of the 16 values provided on the Hamamatsu datasheet for each array. This  $V_{op}$  was adjusted at the actual time of measurement for the ambient temperature using the Breakdown Voltage ( $V_{br}$ ) vs Temperature coefficient of 56 mV/°C (provided by Hamamatsu).

Each sample was given an initial visual inspection to check for any physical damage. Several samples were also checked for conformity to the dimensions shown in Figure 1. Other than an occasional dust mote on the optically sensitive surface, all samples appeared free of any visually obvious defects. All 80 samples were characterized in terms of PDE, Gain, Dark Rate, and Cross Talk. Visual inspection of the output pulses indicated that the SiPM arrays met the Pulse Characteristic specifications (Table 1).

It should also be noted that the relatively soft pins of the device make it imperative that the device be inserted or removed from a socket with great care as the pins are relatively easy to bend. A custom tool is being made for future use to allow for consistent and correct handling of the device when connecting to a readout socket.

## Characterization Measurements of the Samples:

Figure 2 shows the custom readout board which allowed each of the 16 cells to be readout simultaneously. Each output also included a  $\times 66.7$  gain pre-amplifier to provide a clear resolution of the individual photoelectron peaks in the QDC charge spectra. Figure 3 shows the setup used to characterize the performance of the devices. A modified version of the setup (Figure 4) was used to calibrate the actual photon flux. This was needed for the measurement of the PDE of the device. A high-speed VME-based data acquisition system provided a relatively rapid accumulation of data (2 kHz per channel with 3 minute runs as typical). This system used a Wiener USB controller module in association with a CAEN V792 32-channel QDC. (The V792 QDC provides a charge resolution of 100 fC per QDC bin thereby allowing one to measure the Gain from the peak-to-peak charge separation in the QDC spectra.) PC-based software using a custom Labview application provided the interface. To acquire information for the required parameters, five successive runs were made: Dark, 1%, 2%, 4%,

and 6% of full intensity (as determined in the setup of Figure 4). The temperature was stable enough to allow only a single  $V_{op}$  (tuned to that temperature) for all 5 runs. The current draw under dark conditions was also acquired for future analysis of Dark Rate versus Dark Current. This also allowed for the verification of the actual operating Overbias above the Breakdown Voltage. *For the entire sample set, the average Overbias was found to be  $0.90 \pm 0.03$  volts.* Figure 5 shows an example set of QDC data for a single cell from an array.

Using the calibration setup of Figure 4, the actual full (100%) intensity was determined to be 13 photons/mm<sup>2</sup>. The filtered intensities assured that only a relatively small number of pixels were being activated thereby maintaining a linear range of operation. A variety of intensities allowed one to check the consistency of the individual measurements. A data analysis method was developed to use all of the input data from the different runs. The distance between the peaks is proportional to the intrinsic gain, and the relative distribution of the peaks at different intensities is related to the PDE and Dark Rate. The deviations from a strictly Poisson distribution of peaks can be used to provide the Crosstalk value. (The Crosstalk also includes the influence of Afterpulses. Differentiating between the two will be left to a future study.)

Although temperature could not be actively controlled, the temperature was monitored so that the applied bias could be adjusted accordingly. Furthermore, the laboratory had a fairly stable daily temperature pattern. Figure 6 displays the actual temperatures for each of the samples. Overall this gives an average temperature of  $23.0 \pm 0.4^\circ\text{C}$  during the characterization of the entire sample set.

Figures 7, 8, 9, and 10 display the key results from the current study. Since the temperature distribution during the runs was tightly grouped and was only  $-2^\circ\text{C}$  (on average) below the Hamamatsu standard of  $25^\circ\text{C}$ , all of the displayed results are for the actual temperature taken during the run. In a future study, a special temperature controlled setup will be made so that all results can be normalized to a standard temperature to remove any temperature related deviations. As it is, the results are impressive even without such corrections. In conjunction with Figure 7, Figure 11 shows the distribution of Dark Rates for sample 24, which has a unusually noisy single cell.

As a comparison between Hamamatsu and JLAB, Figure 12 shows the ratio of the average Dark Rates for each of the arrays. Since the JLAB data was collected slightly below the Hamamatsu  $25^\circ\text{C}$  standard, it is to be expected that the average ratio is slightly below 1.0.

Figure 13-16 explore the variation of the key parameters of Dark Rate, Gain, PDE and Crosstalk as a function of the applied bias. It was noticed early on that for the recommended  $V_{op}$ , the Gain was slightly below  $6 \cdot 10^5$ , well below the stated nominal value of  $7.5 \cdot 10^5$ . However, the Dark Current data, some examples of which are shown Figure 17, clearly indicated that the  $V_{op}$  corresponded to an Overbias of 0.9 volts (on average) above the Breakdown Voltage  $V_{br}$ . In addition, the average PDE was measured to be 21%. From previous studies with 1 mm<sup>2</sup> and 3x3 mm<sup>2</sup> samples of the 50  $\mu\text{m}$  device type, these values were seen to be completely consistent with each other. Furthermore, the JLAB specs would also be met. The only question was what would the increase be for the PDE, Dark Rate and Crosstalk at the nominal gain. The PDE increases to 26%, (consistent with past studies), the Dark Rate to 24 MHz, and the Crosstalk to 32%. As well, the Overbias is in the range of 1.2-1.3 volts, also consistent with past work.

Magnetic field tests will be performed in the near future at JLAB. The data from the literature clearly indicates that these devices are immune to strong magnetic fields. The chief concern is that of the magnetic sensitivity of the associated electronics and materials that are added to the device. The

expectation is that these will be immune to the high fields ( $< 2$  T) that will be present in the installed location. The final set of magnetic immunity studies will take place in the near future.

Radiation tolerance has already been studied and a prescription has been made that should allow the devices to last the full 10 year lifetime of the experiment. Further tests may be carried out to provide specific parameters associated with these newer versions of the array, especially as they displayed a significantly lower (x4) initial dark rate than the original prototype sample set of 10 samples.

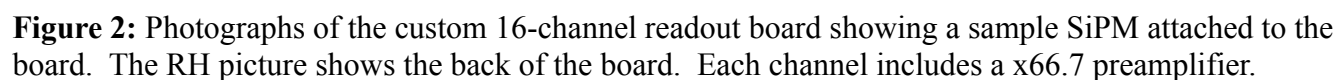
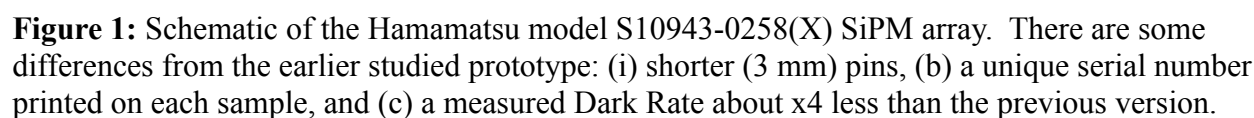
Radiation tolerance studies are ongoing. Some initial results are shown in Figure 18. For now, it appears that the lower dark rate does not affect the damage rate. It only acts as a initial value. The Dark Rate rises at the same rate with dose as with the previous, more noisier prototype array.

**Table 1**

	<b>Property</b>	<b>Specification</b>	<b>Comment</b>
1	Gain @ Vop	$(0.5 - 2.0) \cdot 10^6$	√
2	Photosensitive Area	$> 140 \text{ mm}^2$	√
3	Macroscopic Active Area	$> 75\%$	√
4	Number of microcells	$> 56,000$	√
5	Sensitivity to Magnetic Fields	$< 1\%$ change @ 2T – independent of orientation	Note 1
6	PDE	$> 19\%$	√
7	Dark rate	$< 100 \text{ MHz}$	√
8	Dark Current	$< 40 \text{ mA}$	√
9	Temperature sensitivity	$< 10\%$ Charge Amplitude per $^{\circ}\text{C}$	√
10	Output difference among cells of an array	$< 7.5\%$	√
11	Variation of output among all arrays (using array average)	$< 5\%$	√
12	Nominal operating voltage (Vop)	25 – 80 V	√
13	Nominal Bias above Breakdown Voltage	0.9 – 3.0 V	√
14	Fraction of multiple photoelectrons in Dark Noise	$< 5\%$	√
15	Package Dimensions	Drawing K30-F10530	√
16	Package substrate	$\text{Al}_2\text{O}_3$	√
17	Inputs	4 Bias voltages	√
18	Outputs	16 outputs	√
19	Output connector	Cu alloy pins on 0.05" centers	√
20	Rise time (10%-90%)	$< 16 \text{ ns}$	√
21	Pulse width (10%-10%)	$< 100 \text{ ns}$	√
22	Sensitivity of signal-to-noise to radiation	$< 1\% / \text{Gy}$	Note 2

**Note 1:** Fully equipped units will be tested in near future. The literature is clear that the devices are immune to magnetic fields ( $< 7 \text{ T}$ ). Although expected to be immune, there is a need to check the associated electronics and materials of the readout system.

**Note 2:** Tests of earlier prototypes have already resulted in prescription to allow devices to last expected experimental lifetime of 10 years. Further tests will provide some specific data associated with these newer and much less noisier devices.



## JLAB SiPM Characterization Workstation

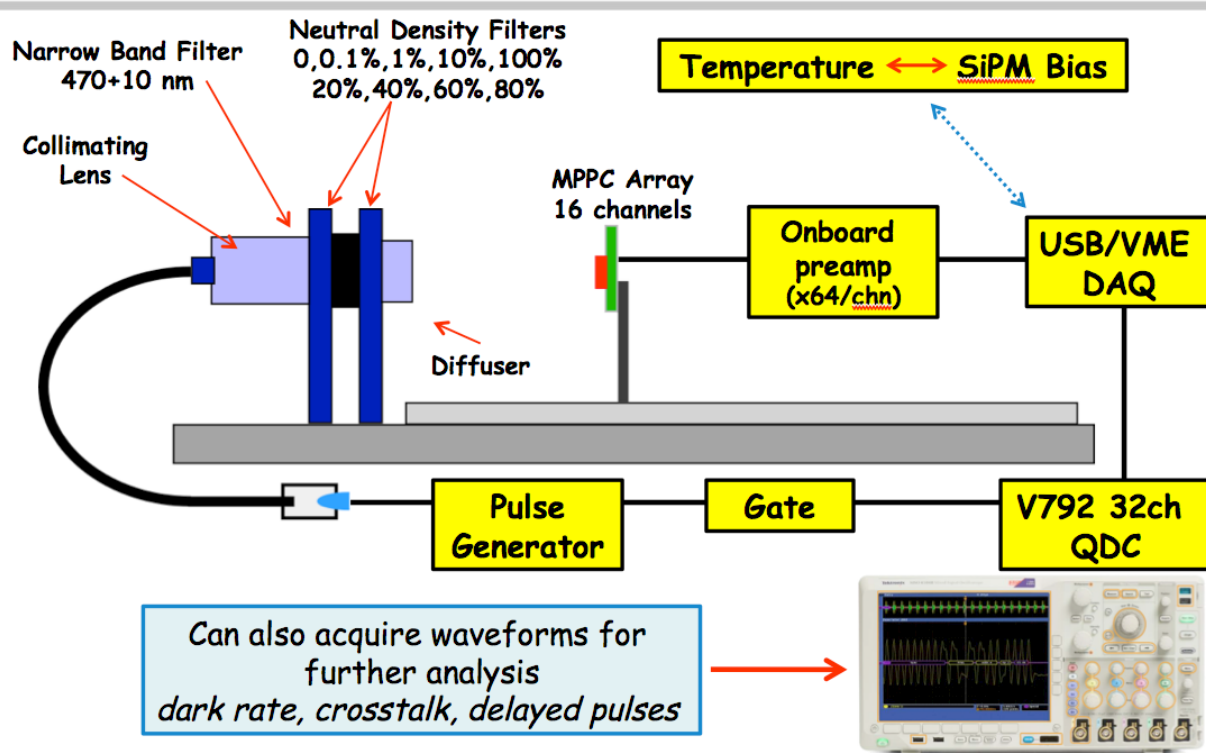


**Figure 3:** Setup to characterize the performance of the 1<sup>st</sup> Article samples. A blue LED filtered at 470 nm provided a fast pulsed light source. The wavelength of 470 nm corresponds to the mean wavelength from the BCAL scintillator. The lens and diffuser provide a method to uniformly illuminate the sample array. The sets of neutral density filters allowed one to precisely control the intensity of illumination. Temperature was monitored to allow for slight adjustments in the operating voltage using the coefficient of 56 mV/°C (relative to the  $V_{op}$  at 25°C). An acquisition rate of 2 kHz was sufficient to gather sufficient statistics for several levels of intensity: Dark, 1%, 2%, 4%, and 6% (of the full intensity of 13 photons per mm<sup>2</sup>). A long gate of 1  $\mu$ s allowed for acquisition of additional delayed afterpulse information. The oscilloscope will also be used in future studies of afterpulse analysis.

## JLAB Workstation – Light Source Calibration

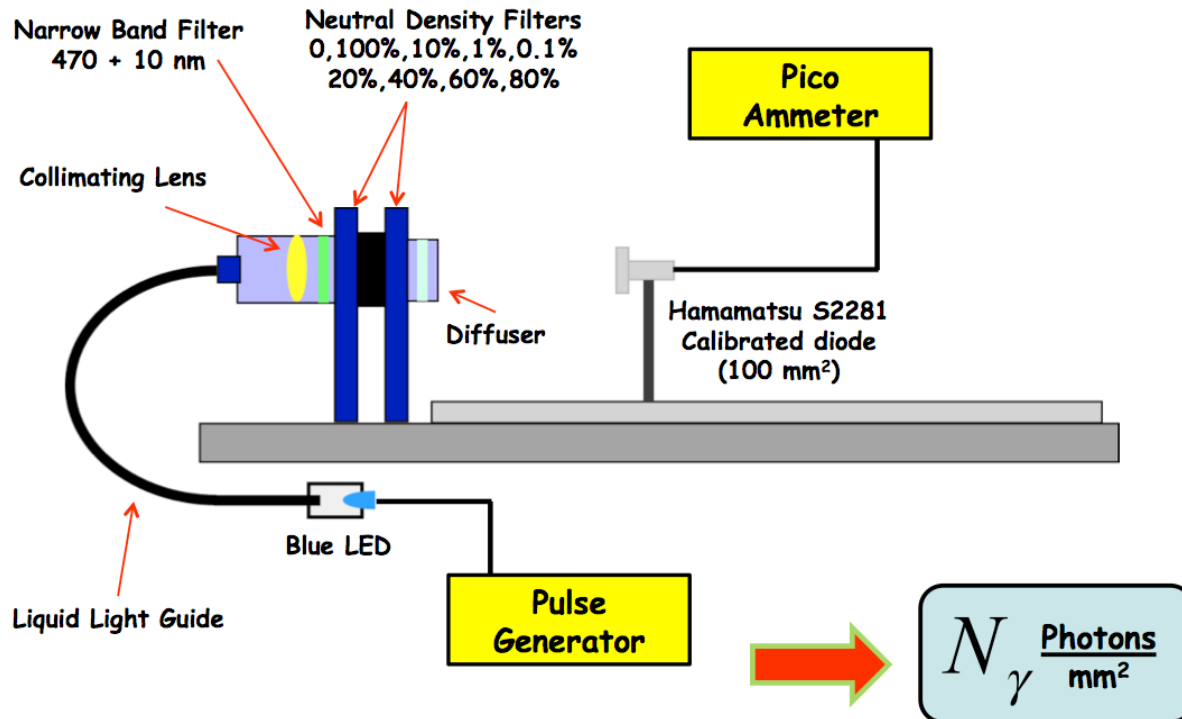


**Figure 4:** Setup for calibration of light intensity (photons per mm<sup>2</sup>). The pulse generator was varied in frequency (1 kHz – 2 MHz) to create an increasing set of currents (with no intensity filters). When plotted as Current vs Frequency, the slope of this linear data set is proportional to the photon intensity using the fact that (a) the photodiode is calibrated in quantum efficiency, (b) the photodiode gain is unity, and the (c) calibrated area of the photodiode is 100 mm<sup>2</sup>. The intensity was determined to be 13 photons per mm<sup>2</sup>.



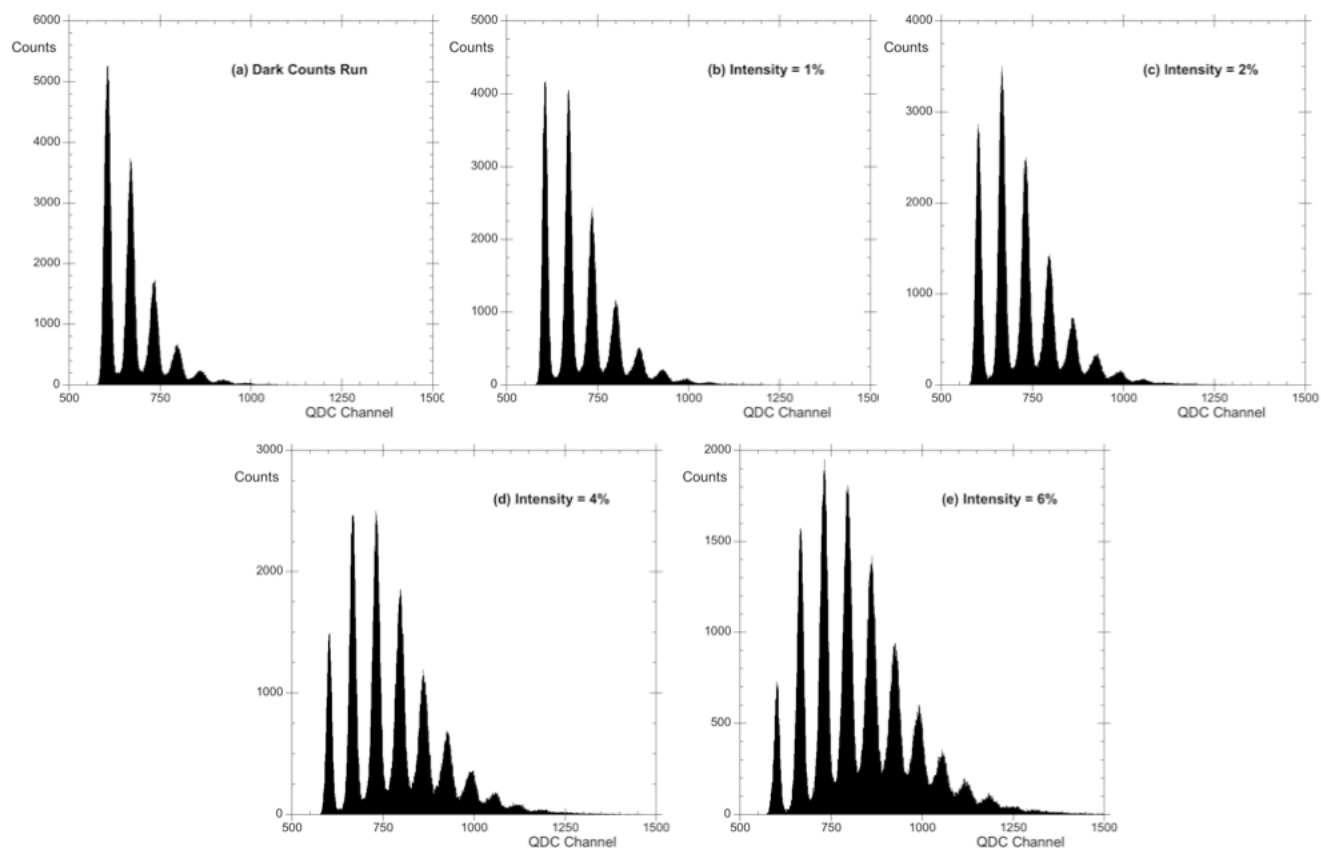


**Figure 5:** Examples of typical QDC data for one cell (3x3 mm<sup>2</sup>) from a SiPM array.

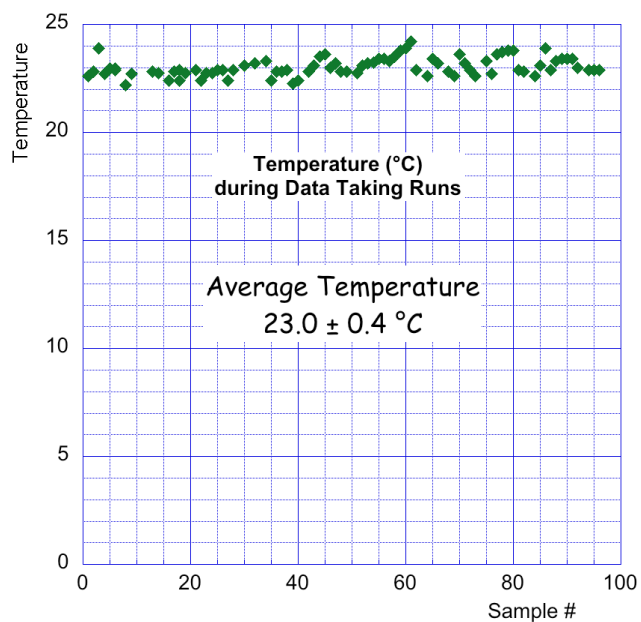


**Figure 6:** Temperature during actual data runs for all 1<sup>st</sup> article samples.

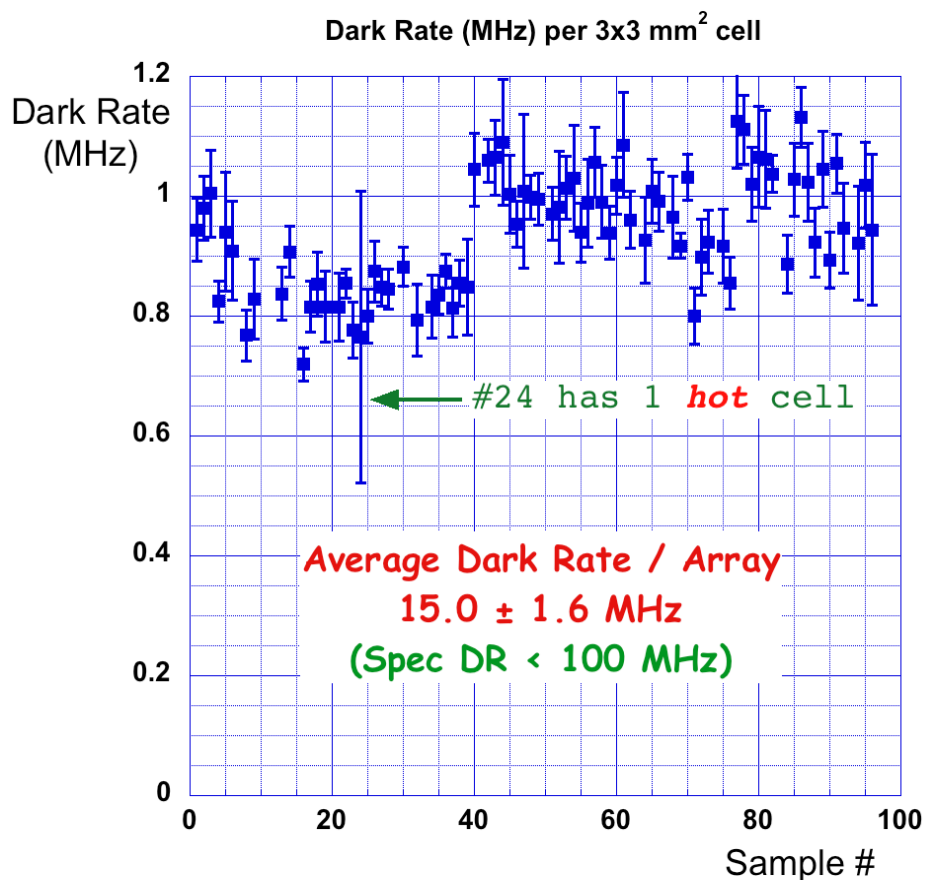


**Figure 7:** For each sample, the average Dark Rate per 3x3 mm<sup>2</sup> cell. The error bars indicate the variation of the Dark Rate for that sample array. Sample 24 is notable for having an one very high dark Rate cell which creates the large error bar. Figure 11 (below) shows the Dark Rates for that sample displaying both the Hamamatsu and JLAB data. Scaling the overall results to the arrays, one finds the average Dark Rate per array to be 15 MHz – well below the original specification of 100 MHz. Using the variable bias data displayed in Figure 15, the Dark Rate at the nominal gain of  $7.5 \cdot 10^5$  becomes 24 MHz, still well within the specifications.

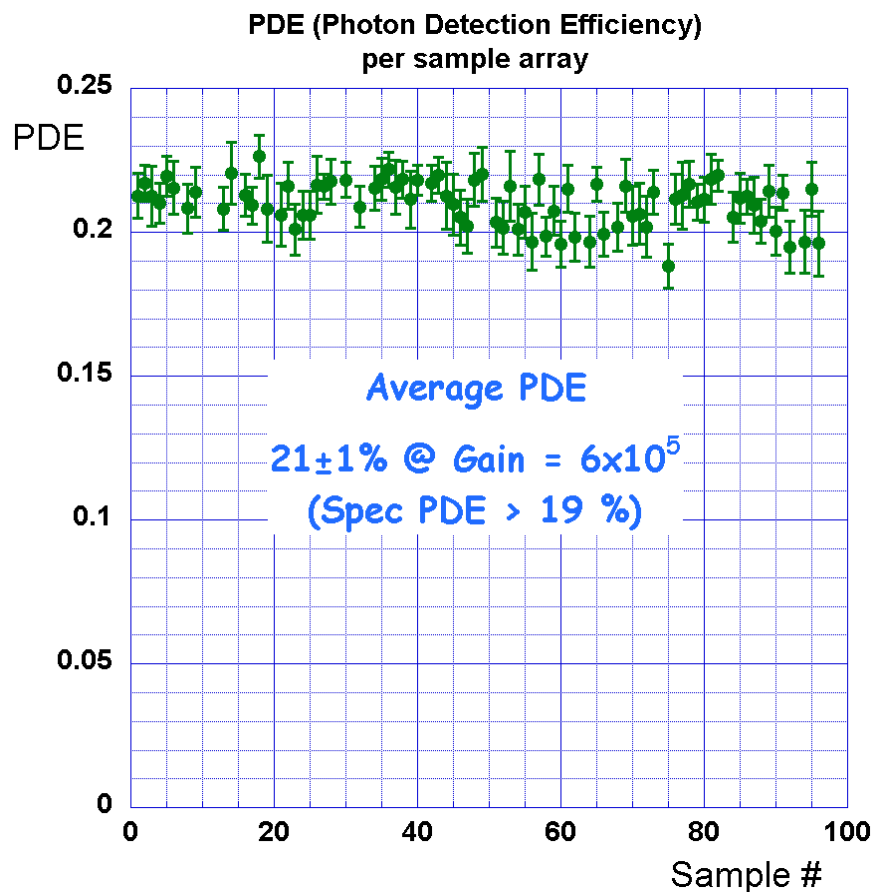


**Figure 8:** Average PDE of all cells for each of the samples. The average PDE for the average Gain ( $6 \times 10^5$ ) is 21%. The error bars represent the variation in the PDE among the 16 cells of each array. The average variation within an array is 4%. Over the 80 samples, the average PDE varies 3.6%. Using the variable bias data from Figure 14, the average PDE rises to 26% for a nominal Gain of  $7.5 \times 10^5$ .

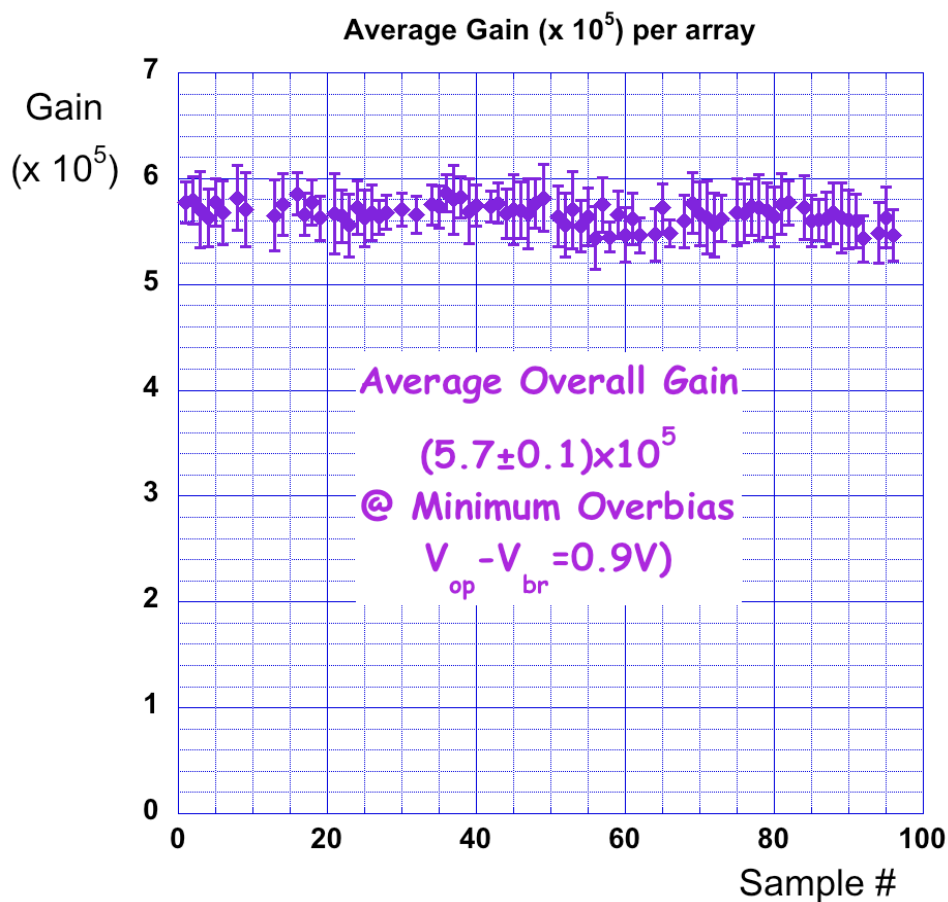


**Figure 9:** Average Gain for all 16 cells of each array. The error bars show the variation in the Gain among the 16 cells of each array. The uniformity of the gain within an array is an average of 4.5%. Among the 80 samples, the average gain varies by only 1.7%. IV data shows that the  $V_{op}$  corresponds to an Overbias of 0.9 volts above the Breakdown Voltage ( $V_{br}$ ). The average Gain and Overbias are consistent with the Hamamatsu datasheets for the 50  $\mu m$  microcell model of SiPM.

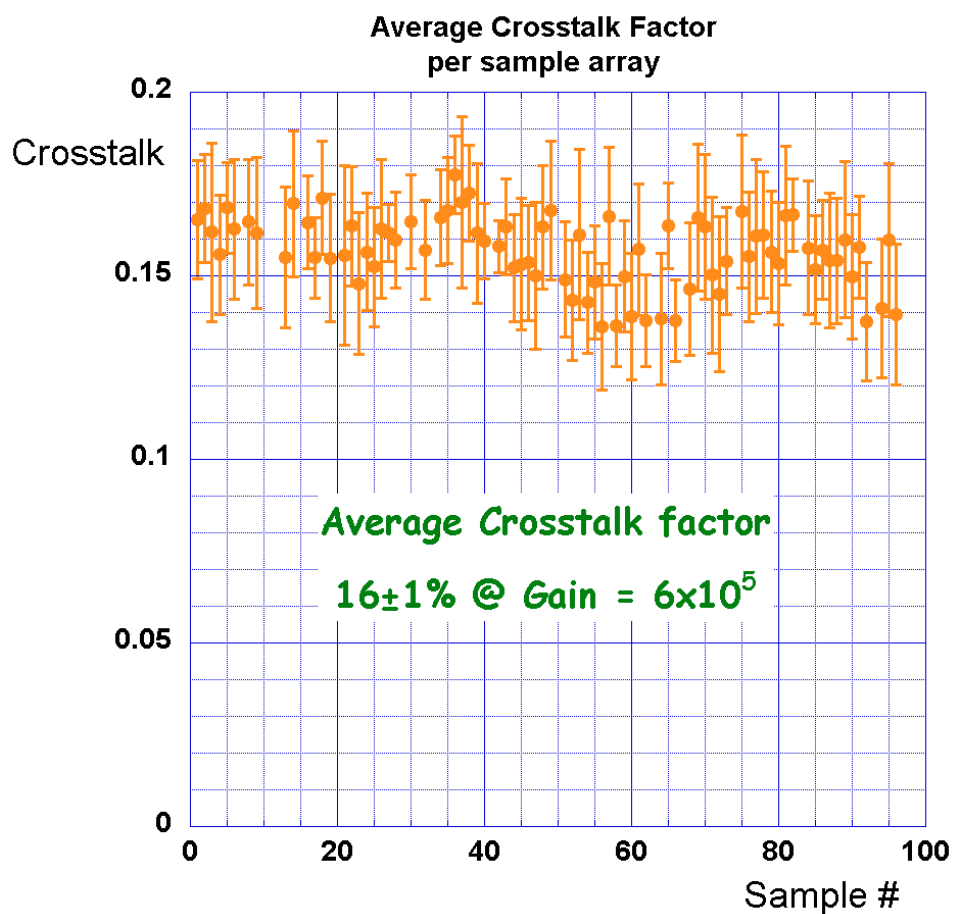


**Figure 10:** Average Crosstalk factor for all 16 cells of each sample array. The variation among the 16 cells of an array is represented by the error bars. The overall average is 16% at the measured Gain of  $6 \times 10^5$ . At the nominal Gain of  $7.5 \times 10^5$ , the factor rises to 32%.

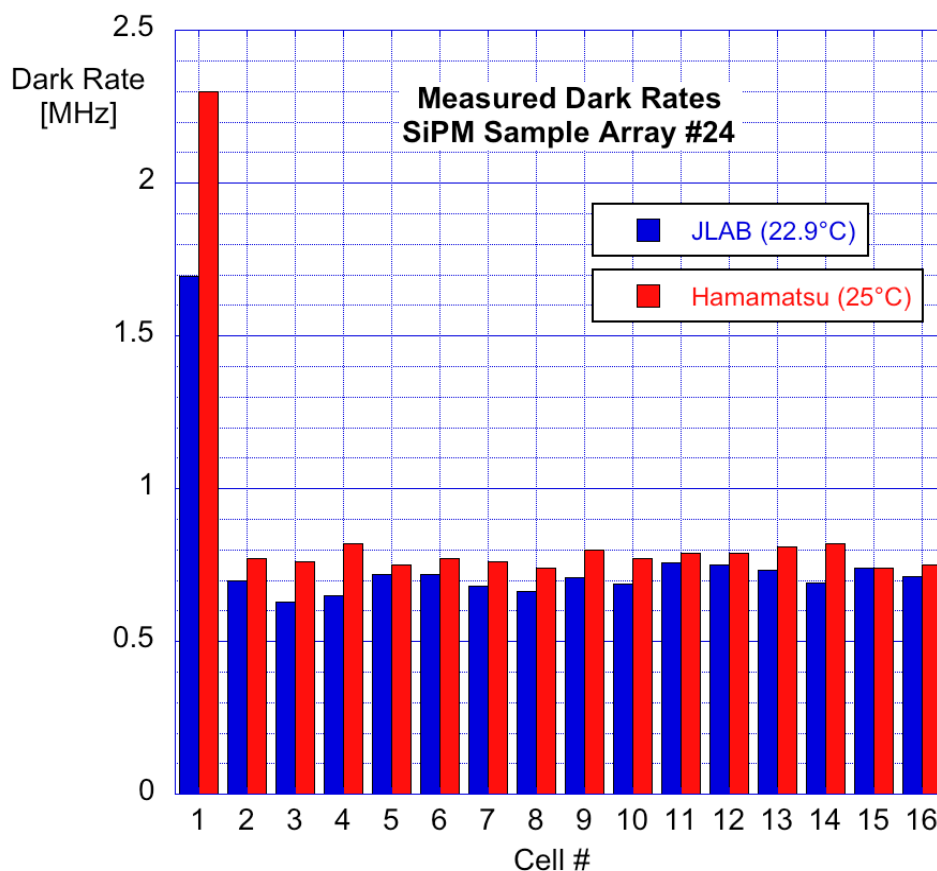


**Figure 11:** Measured Dark Rates for SiPM #24 showing the one “hot” cell in an otherwise low noise array. Note that this does not adversely affect PDE, Gain and Crosstalk for the sample.

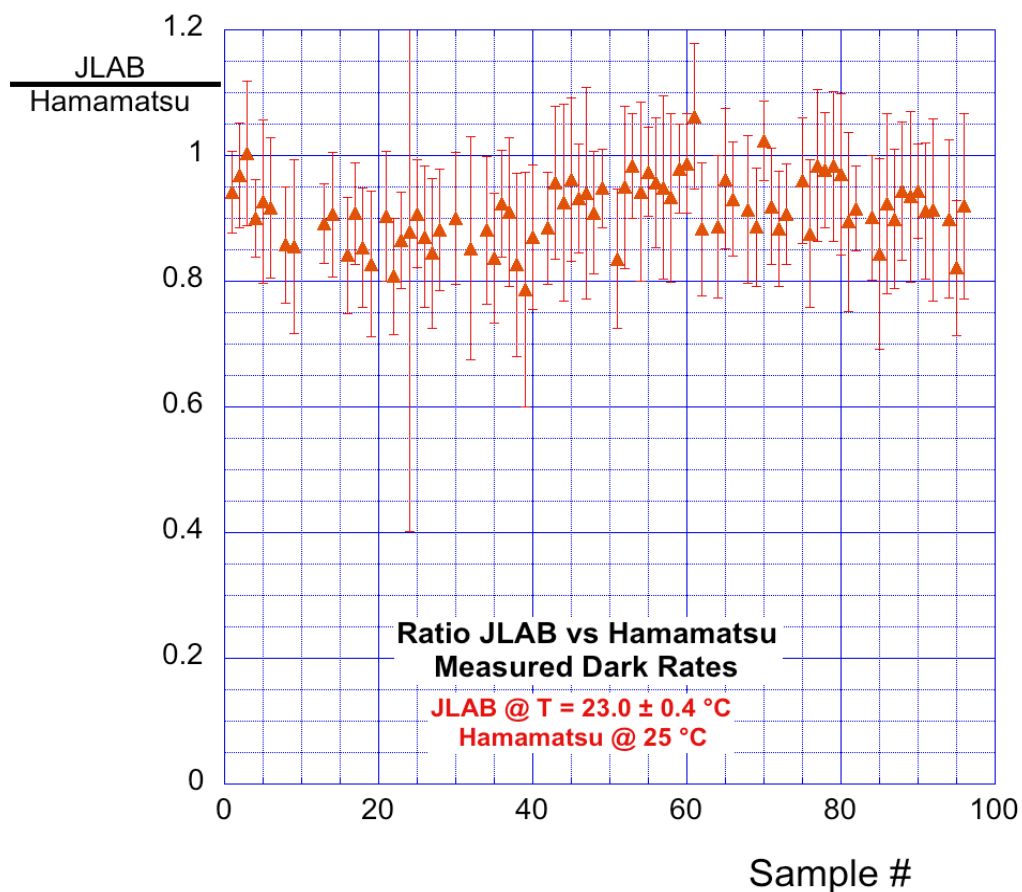


**Figure 12:** Ratio between JLAB and Hamamatsu average Dark Rates. Since the JLAB data was measured at a slightly lower temperature, the average ratio of  $0.91 \pm 0.05$  is consistent with expectations.

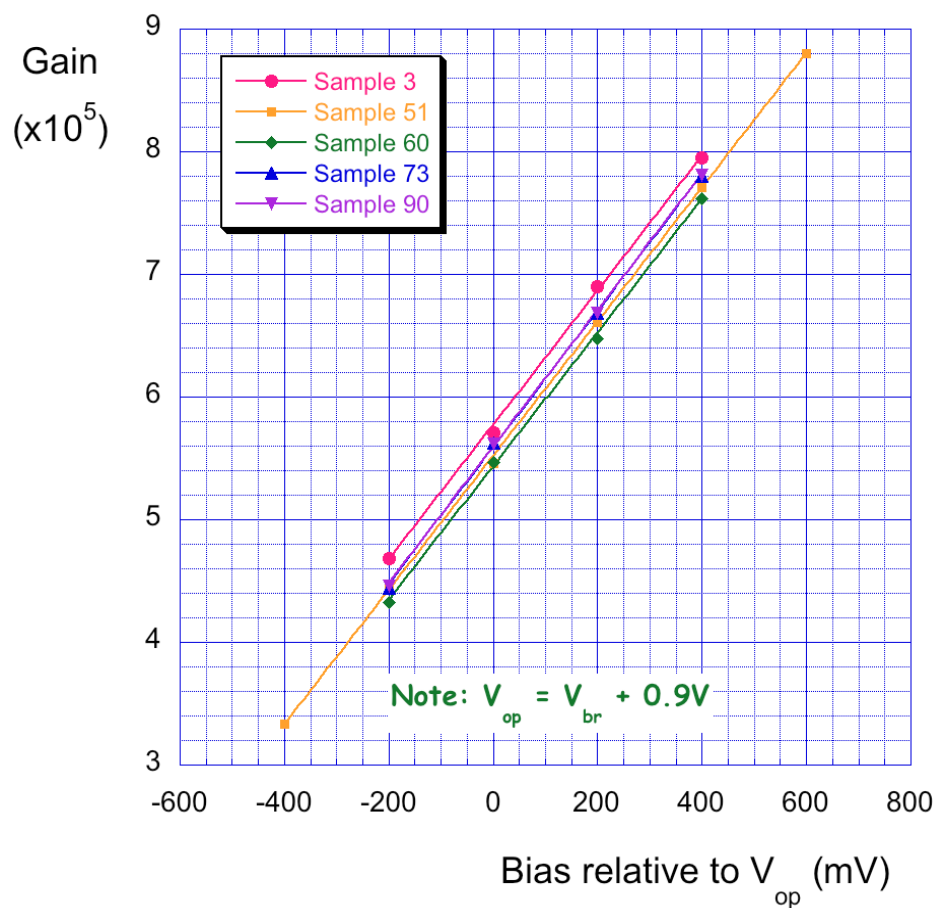


**Figure 13:** Gains of several samples operated over a range of bias. Note that the nominal gain of  $7.5 \cdot 10^5$  corresponds to about 0.35V above  $V_{op}$ , which is consistent with the Hamamatsu data on the 50  $\mu\text{m}$  device.



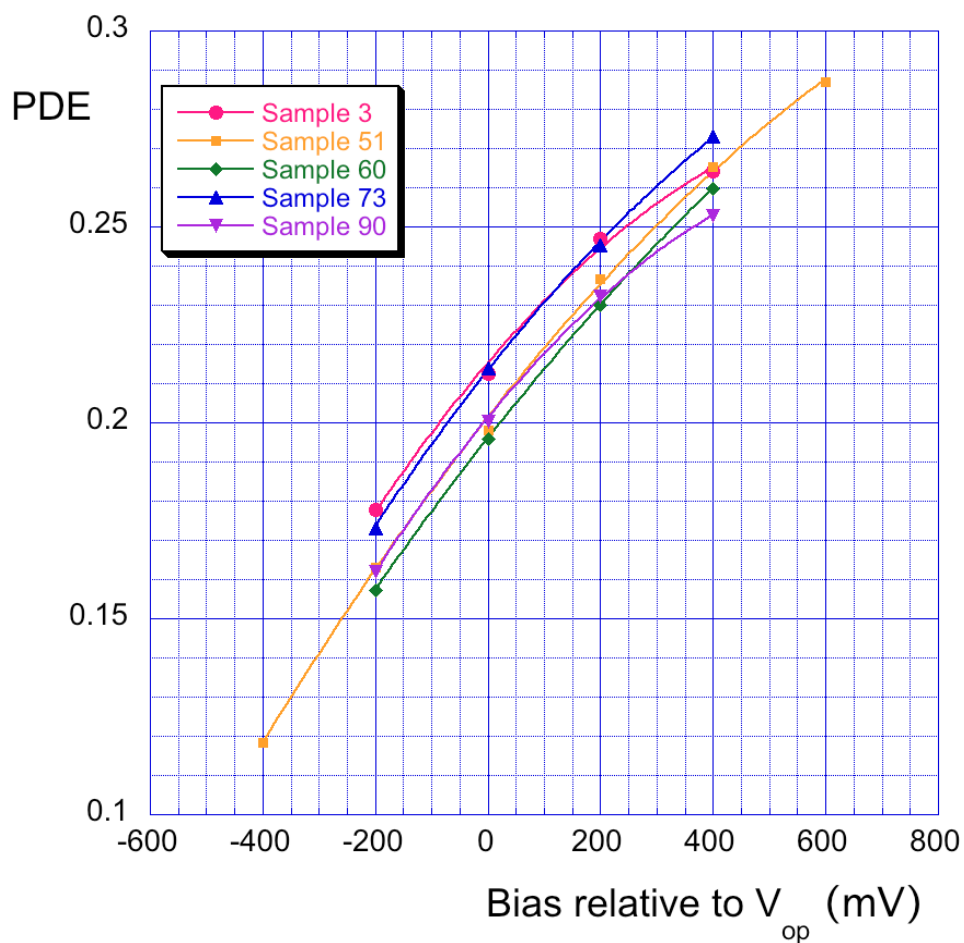


**Figure 14:** Variation of PDE with the applied bias. From this one can see that the PDE at the nominal Gain of  $7.5 \cdot 10^5$  would be about 25-27%, consistent with earlier results with small  $1 \text{ mm}^2$  samples of the  $50 \text{ }\mu\text{m}$  device. The slight non-linear behavior will be explored in future studies. One can speculate that it is related to the non-linear increase in Crosstalk seen in Figure 16.

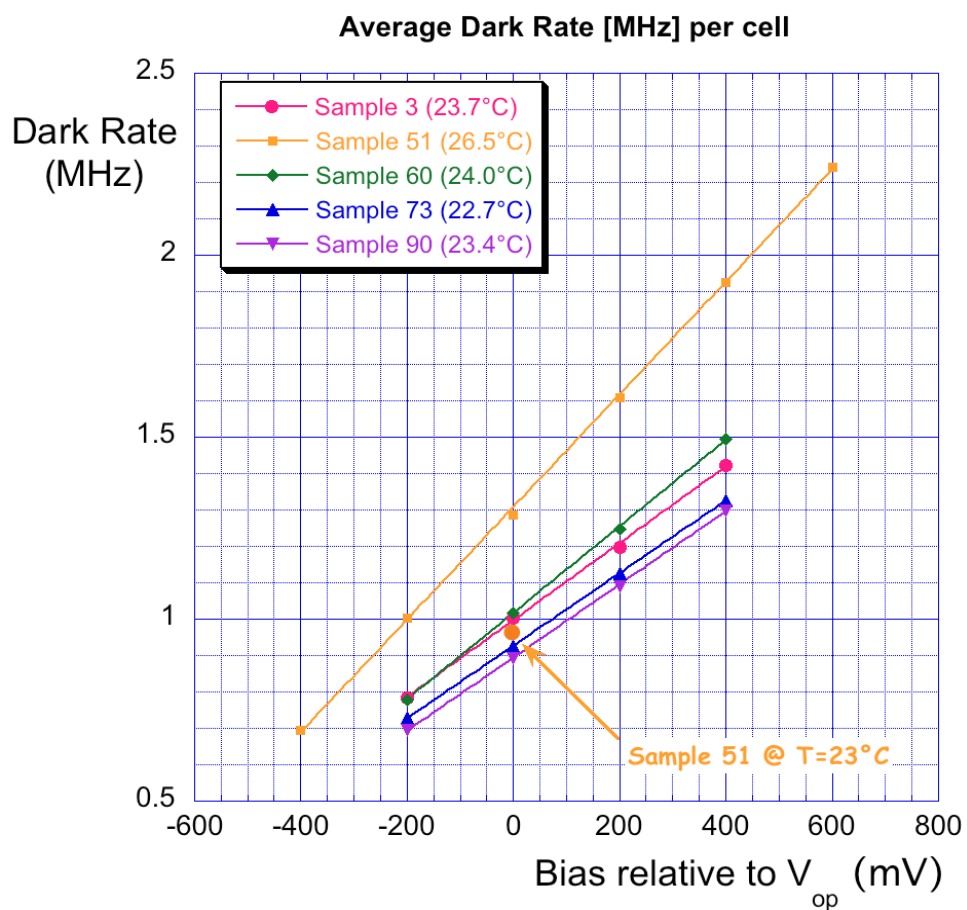


**Figure 15:** Average Dark rate (per cell) for variable applied bias. Note that the data for sample 51 was taken at 2 temperatures – the nominal 23°C and at the elevated temperature of 26.5°C. The plot indicates that for a nominal Gain of  $7.5 \cdot 10^5$ , the average Dark Rate for an array will be in the range of 21-24 MHz.

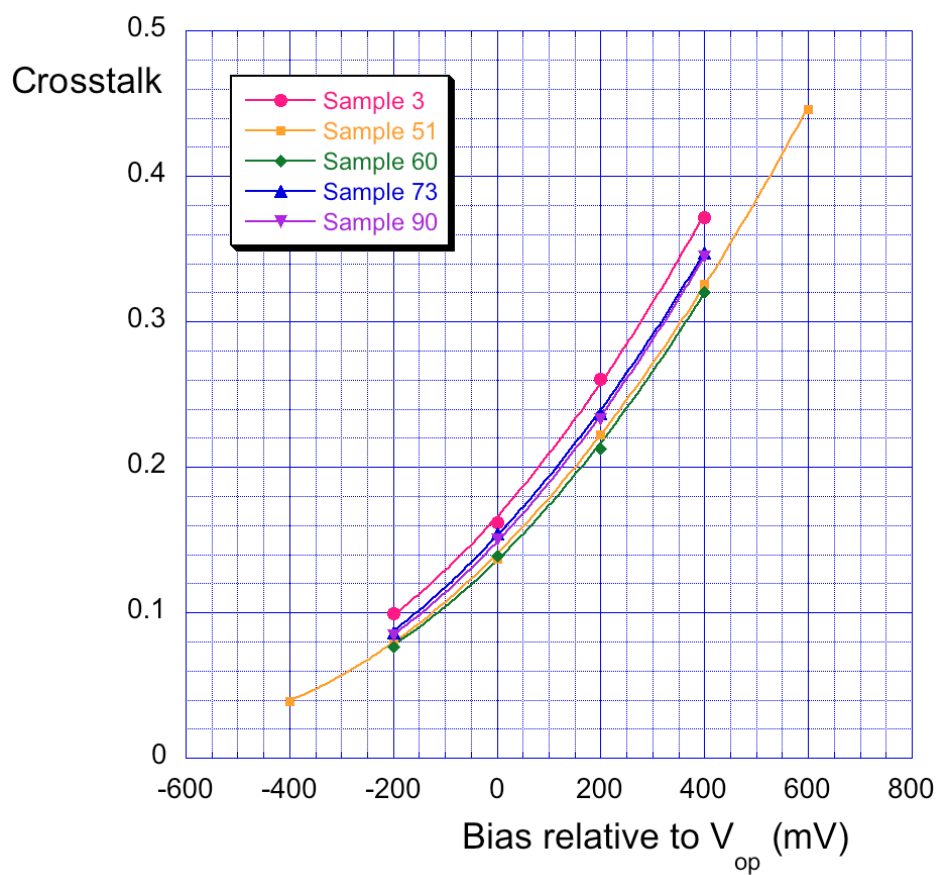


**Figure 16:** Average Crosstalk as a function of applied bias.

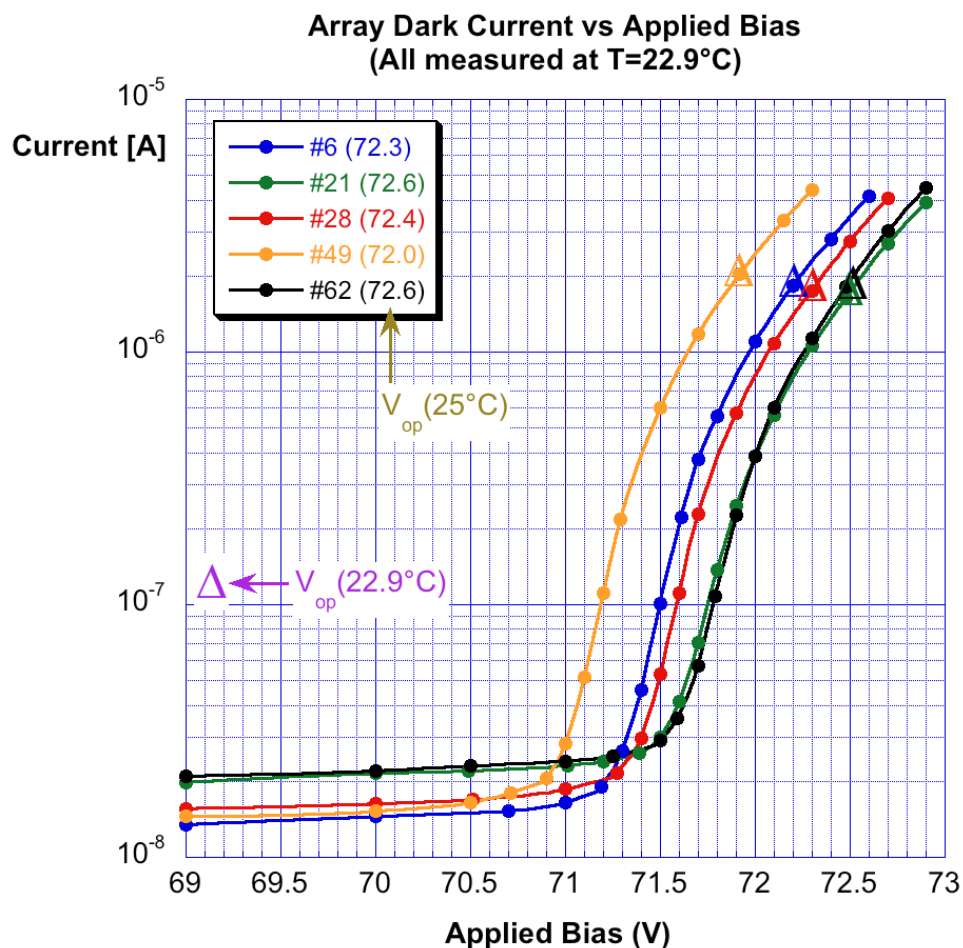


**Figure 17:** Examples of Dark Current data for several arrays that were operated at the same temperature. Both the Hamamatsu  $V_{op}$  and the actual bias are displayed. As noted in the text, the average overbias (bias above breakdown voltage) was found to be 0.9 volts for the full sample set of 80 arrays. The triangle symbols represent the actual  $V_{op}$  used for the measurement at the stated temperature of  $22.9^{\circ}\text{C}$ . The standard  $V_{op}$  (for  $25^{\circ}\text{C}$ ) is listed next to each sample number in the plot legend.

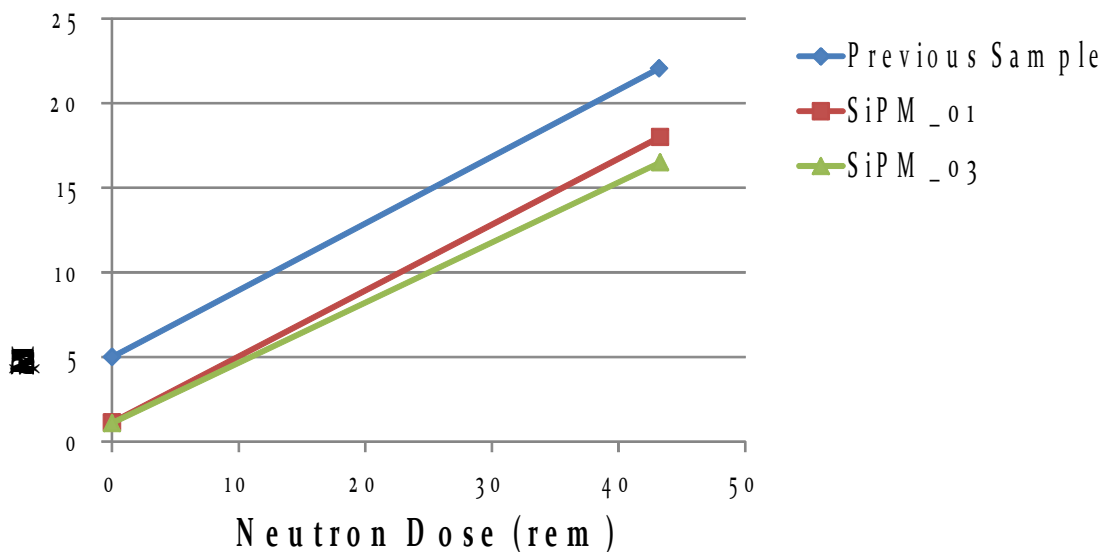


**Figure 18:** Two samples from the 1<sup>st</sup> Article Sample Set were irradiated to the same neutron dose by a AmBe source as a sample from the previously studied prototype array. The dose is equivalent to running at 5 years at high luminosity with a liquid hydrogen target in Hall D (GlueX). As with the previous sample, the two new samples were heated at 40°C after irradiation to achieve a rapid anneal to the residual level of damage. It is this residual damage, as represented by the increase in Dark Current, which is shown in the plot. As can be seen, despite the initially lower Dark Current of the new samples, the slope of the damage curve is the same indicating the amount of damage as a function of dose remains the same for the 1<sup>st</sup> Article Samples.